



Repositorio Institucional de la Universidad Autónoma de Madrid

<https://repositorio.uam.es>

Esta es la **versión de autor** del artículo publicado en:

This is an **author produced version** of a paper published in:

Journal of Porphyrins and Phthalocyanines 24.01n03 (2020): 33-42

DOI: <https://doi.org/10.1142/S1088424619300167>

Copyright: © 2019 World Scientific Publishing Co Pte Ltd.

El acceso a la versión del editor puede requerir la suscripción del recurso

Access to the published version may require subscription

Polar Columnar Assemblies of Subphthalocyanines

Maria J. Mayoral^{*a}, Tomas Torres^{*a,b,c} and David González-Rodríguez^{*a,b}

^a Nanostructured Molecular Systems and Materials (MSMn) and Nanoscience and Molecular Materials groups.
Departamento de Química Orgánica, Facultad de Ciencias, Universidad Autónoma de Madrid, 28049 Madrid, Spain.

^b Institute for Advanced Research in Chemical Sciences (IAChem) Universidad Autónoma de Madrid, 28049 Madrid, Spain.

^c IMDEA Nanociencia, c/ Faraday 9, Campus de Cantoblanco, 28049 Madrid, Spain.

Received date (to be automatically inserted after your manuscript is submitted)

Accepted date (to be automatically inserted after your manuscript is accepted)

ABSTRACT: In this small review article, we provide an overview of the different self-assembled systems and materials created so far by rationally organizing fluoroSubPcs in a non-centrosymmetric fashion, which allows access to novel polarly ordered liquid crystalline materials that can be aligned in the presence of electric fields and that exhibit permanent or switchable (*i.e.* ferroelectric) polarization.

KEYWORDS: Subphthalocyanines, Porphyrinoids, Supramolecular Chemistry, Self-assembled Materials, Ferroelectric Liquid Crystals.

*Correspondence to: Prof. David González-Rodríguez, Departamento de Química Orgánica, Facultad de Ciencias, Universidad Autónoma de Madrid, 28049 Madrid, Spain, +34 91 497 2778, david.gonzalez.rodriguez@uam.es. Prof. Tomás Torres, Departamento de Química Orgánica, Facultad de Ciencias, Universidad Autónoma de Madrid, 28049 Madrid, Spain, +34 91 497 4151, tomas.torres@uam.es. Dr. Maria J. Mayoral, Departamento de Química Orgánica, Facultad de Ciencias, Universidad Autónoma de Madrid, 28049 Madrid, Spain, +34 91 497 5807, maria.mayoral@uam.es.

INTRODUCTION

The self-assembly of planar π -conjugated molecules into stacked wire-like structures, in which these semiconducting discotics strongly interact through their π -electron surfaces along the columnar axis, is considered one of the most promising nanoscale architectures in organic materials^[1-3]. This assembly process, not only in condensed phases^[4], but also in solution^[5], and the properties of the materials obtained, are the basis of manifold applications.

Now, when molecular structure deviates from planarity, as in bowl-shaped discotics^[6], additional exotic properties may arise upon molecular stacking. Firstly, and in contrast to flat discotics, a cone-shaped molecule may show different aggregation modes, since it displays a convex and a concave side. Hence, the supramolecular interaction between two cone-shaped molecules may in principle lead to distinct assembly arrangements, depending if the association takes place between convex sides, concave sides, or a concave-convex association^[7]. Interestingly, only the latter aggregation mode can result in non-centrosymmetric polymeric columns. Second, if one can distinguish two faces, it means that, when properly substituted, a cone-shaped molecule will be chiral^[8], which opens then the possibility for the formation of homochiral helical assemblies^[9]. Interestingly, chirality intrinsically resides here in the core of the molecule, in contrast to the many examples of helical discotic stacks where stereogenic centers are present in peripheral tails^[10]. Finally, a cone-shaped molecule may be endowed with an axial dipole. Upon columnar aggregation, these dipoles may add up along the column resulting in spontaneously polarized materials, potentially able to interact with external electric fields and to produce ferroelectric behaviour. The field of supramolecular ferroelectrics is experiencing a renovated impulse, and novel materials with exotic and promising properties, developed from molecular design, are targeted^[11].

A prominent class of π -conjugated cone-shaped molecules is represented by the subphthalocyanine (SubPc) family^[12]. In comparison with phthalocyanines, these molecules comprise three isoindole units (instead of four) condensed around a boron atom. Due to the smaller macrocycle size and the presence of the boron center, SubPcs are forced to adopt a non-planar cone-shaped structure that still preserves π -aromatic character^[13]. However, in contrast to many of the cone- or bowl-shaped π -conjugated molecules available (sumanene, coronene, calixarene, cyclotrimeratrylene, etc.), which exhibit relatively fast bowl inversion^[14], the cone structure in SubPcs is rigid. This is due to the tetrahedral coordination of the central boron atom to the three isoindoles and to a ligand, which lies at the axial position and is responsible for much of the versatile SubPc reactivity^[15]. Because cone inversion is not allowed, these unique molecules are endowed with permanent axial dipoles and their enantiomers show no racemization, so they could be regarded as potential candidates for the development of polar materials if adequately stacked in non-centrosymmetric columns. Unfortunately, most axial ligands used in SubPcs are too bulky and efficiently prevent columnar aggregation, which has been on the other hand beneficial in many of the applications of these magenta dyes in the fields of nonlinear optics^[16], photodynamic therapy^[17], artificial photosynthetic mimics^[18], or organic optoelectronics^[19]. There has been so far one exception: a fluorine axial atom, whose size is small enough to allow, as will be explained below, the formation of non-centrosymmetric columns upon concave-convex stacking interactions between SubPc cores.

In this small review article, we provide an overview of the different self-assembled systems and materials created so far by rationally organizing fluoroSubPcs in a non-centrosymmetric fashion, which allows access to novel exciting properties that are related to polar order. As a matter of fact, the concave-convex stacking of these tetrahedral-shaped axially dipolar molecules results in materials that can be aligned in the presence of electric fields and that exhibit permanent or switchable polarization.

Columnar aggregates based on SubPcs in the solid state

As stated above, due to the fact that SubPcs are rigid, aromatic, non-planar macrocycles with a permanent dipolar moment in the axial direction, they can be thought as extraordinary candidates to occupy the rigid core in columnar structures. Nevertheless, the organization of these unique molecules in columns constitutes in itself a challenging enterprise owing to the presence of the axial substituent, which hampers the development of strong π - π interactions. In a collaborative publication Gutiérrez-Puebla, Elguero, Torres and co-workers developed new methods to incorporate a fluorine atom at the axial position of SubPcs and found that these molecules could form antiparallel stacked columnar structures in the solid crystalline state^[20]. The molecular packing of SubPc **1** is extremely tight, with unusually short intermolecular F \cdots N distances between contiguous molecules (1.4 Å, Fig. 1). This was the first time that such organization was observed in SubPcs, and the authors attributed this result to the low steric volume of fluorine in comparison with typical axial groups.

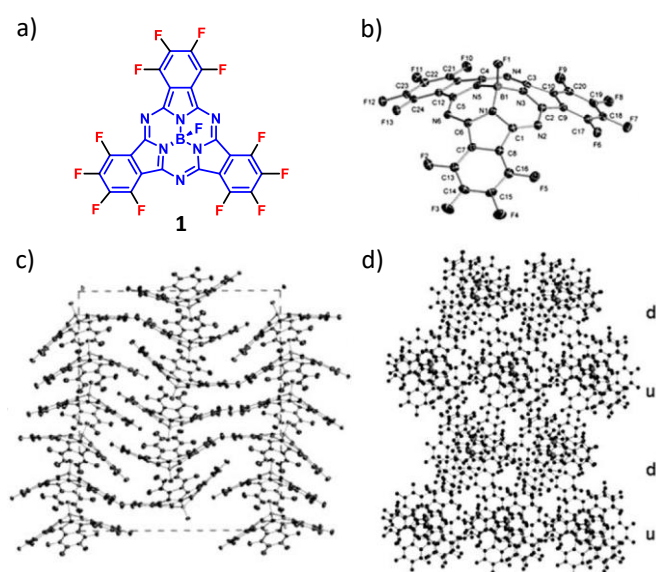


Fig. 1. (a) Structure of SubPc **1**. (b) Molecular structure showing thermal ellipsoids at the 50% probability level of **1**. Views showing (c) the columns along the *c* axis and (d) the columns packing along the *ab* plane of **1** (u=up, d=down). Hydrogen atoms were omitted for clarity. Reproduced with permission from ref. [20]. Copyright 2008 Wiley-VCH Verlag GmbH&Co. KGaA.

This columnar organization was also described by Shimizu, Kobayashi *et al.* in the solid state for core-expanded SubPcs (Fig. 2a)^[21,22]. The π -extended biphenyl moiety incorporated in the SubPc displays a large tilt, which causes helicity of the seven-membered-ring unit, enabling SubPc **2** to exist as *P* and *M* enantiomers. These enantiomers stack alternatively in the molecular packing to form one-dimensional columnar nanostructures as a result of π - π interactions, which are enhanced by the small fluorine axial ligand (Fig. 2b-d). The distorted structure of **2** led to a unique conjugated system, which enabled studies of the aromaticity of the convex and concave surfaces, and induced novel properties, such as a marked split of the *Q*-band absorption at 682 and 510 nm.

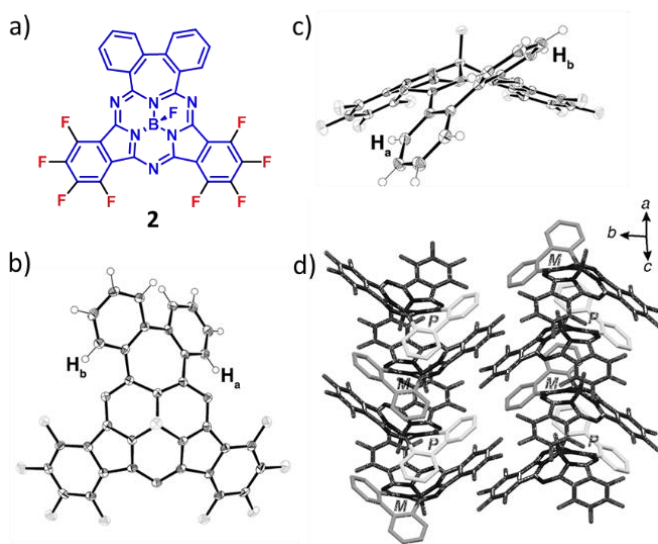


Fig. 2. (a) X-ray single-crystal structure of **2**; (b) side view, (c) top view, (d) packing diagram. The thermal ellipsoids were scaled to the 50% probability level. In the packing diagram, the biphenyl units of the *P* and *M* enantiomers are highlighted. Reproduced with permission from ref. [21]. Copyright 2014 Wiley-VCH Verlag GmbH&Co. KGaA.

Supramolecular self-assembly of SubPcs in solution

Motivated by the results obtained in the solid state, in 2015, Ortí, Torres, González-Rodríguez and co-workers reported the first example of SubPcs able to self-assemble into non-centrosymmetric homochiral supramolecular polymers in solution^[23]. The main driving force for stacking in solution was hydrogen-bonding between amide groups, placed at the periphery of the macrocycle. The tetrahedral-shaped C_3 -symmetric SubPc **3** was synthesized as a racemic mixture and then separated by analytical chiral HPLC as two enantiomers: **3a** and **3b** (Fig. 3a)^[24]. The self-assembly process was studied in apolar solvents by different spectroscopic techniques (UV-vis absorption, emission and CD) and the observed spectral features clearly indicated the formation of head-to-tail columnar nanostructures (Fig. 3b-d). In particular, compound **3** displayed blue-shifted absorption, a significantly quenched emission, and a different CD spectrum upon aggregation, which is a mirror image for each enantiomer. Temperature-dependent UV-vis experiments of **3a/b** in MCH, in combination with theoretical calculations, established that the columnar SubPc assemblies are formed through a highly cooperative supramolecular polymerization process driven by a combination of noncovalent interactions: H-bonding, π - π interactions and dipolar interactions between axial dipolar B-F bonds (Fig. 3b). On the other hand, AFM and TEM measurements confirmed the formation of the proposed supramolecular nanostructures. As shown in Figs. 3e,f long fibrillar objects of 2.5 nm in diameter, along with fiber bundles (5-6 nm), were observed. Additionally, SEM images of a xerogel, prepared by vacuum-drying dodecane gels, revealed an extended and interconnected fibrous network (Figs. 3g,h).

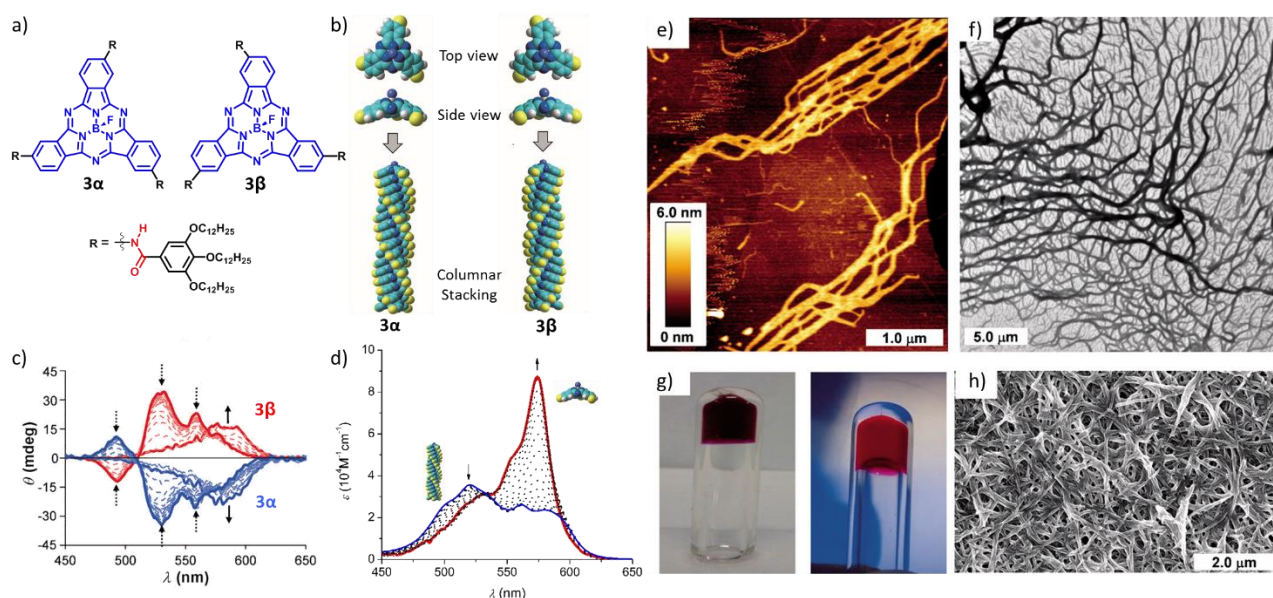


Fig. 3. (a) Molecular structure of the α and β enantiomers of SubPc **3**. (b) Top and side views of the two enantiomers of SubPc **3** and the corresponding homochiral head-to-tail columnar assemblies. Temperature-dependent CD of 3α and 3β (c) and UV-vis of 3α (d) experiments in MCH at $3.9 \cdot 10^{-6}$ M. The absorption features of 3β are identical. Arrows indicate the trends with increasing T values, which leads to deaggregation. (e) AFM height image of SubPc **3** onto HOPG ($3.2 \cdot 10^{-6}$ M, MCH). (f) TEM image of a negatively stained solution of **3** in MCH on a carbon-coated copper grid. (g) Dodecane gels of **3** under no (left) or UV irradiation (right, $\lambda = 365$ nm). (h) SEM image of the corresponding xerogel. Adapted with permission from ref. [23]. Copyright 2015 Wiley-VCH Verlag GmbH&Co. KGaA.

The experimental outcomes were supported by extensive quantum-chemical calculations^[23,35]. On the basis of these studies a right-handed helical stack, in which the conformation of the diarylamide is *anti-in* (see Fig. 4a), promotes the coexistence of intermolecular H-bonding, π - π and dipolar interactions (Fig. 4b-c). It is important to highlight that the calculated F-B contacts between adjacent molecules (2.78 Å) evidences strong dipolar interactions between B-F dipoles along the stacks, as well as the enhancement in stabilization energy per monomer ($\Delta E_{mon,n}$) with an increasing number of monomer units, which suggests a large cooperative character for the self-association process (Fig. 4d).

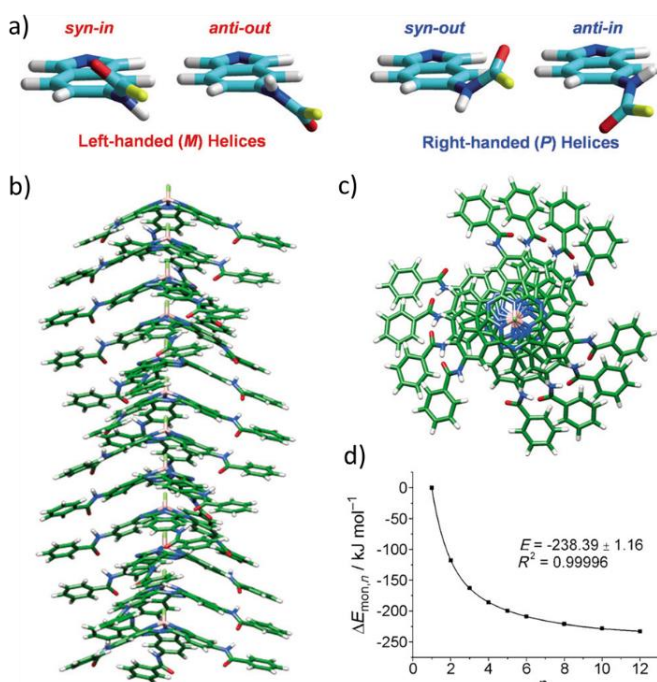


Fig. 4. (a) Amide conformations that can lead to triple intermolecular hydrogen-bonding in the **3β** helical stacks. (b) Side and (c) top views of *P*-helical *all-anti-in* head-to-tail arrangements of **3β** stacks, calculated by DFT. (d) Calculated stabilization energy per monomer unit ($\Delta E_{mon,n}$). Reproduced with permission from ref. [23]. Copyright 2015 Wiley-VCH Verlag GmbH&Co. KGaA.

Liquid crystalline materials with permanent polarization

Thermotropic LCs. The non-centrosymmetric head-to-tail or convex-to-concave columnar organization with a permanent axial dipole moment observed for SubPcs may induce a macroscopic polarization that can result in electric-field-responsive polar materials. With this idea in mind, Sierra, Etxebarria, González-Rodríguez and Torres' labs suggested that SubPcs **3** and **4** (Figs. 3a and 5a) could be considered as extraordinary candidates to be explored as potential mesogens for polar columnar liquid crystalline films^[26,27]. They first explored the thermal properties of **4** by polarized optical microscopy (POM), differential scanning calorimetry (DSC) and X-ray diffraction (XRD). This study showed the formation of a stable Col_h mesophase at room temperature characterized by a pseudo focal-conic texture and a low-angle peak related to the (10) reflection with a cell parameter *a* of 39.0 Å (Fig. 5b-c)^[26]. AFM experiments were in agreement with such intercolumnar distances. Images of the columnar liquid crystalline material onto mica substrates (Fig. 5d) showed that the columns are arranged parallel to the surface, with different domain orientations. Surface analysis revealed a periodicity of 40 Å, which was also in accordance with theoretical PM7 models (Fig. 5c inset). Calculations also suggested that the dipole moment follows the axial B-F stacking axis and systematically increases with the length of the column. In fact, when the stack polarization is arranged parallel to a simulated electric field, the system is stabilized with respect to an antiparallel arrangement. These theoretical calculations already indicated that these SubPc stacks should respond to an electric field and that, if a large number of columns were oriented in the same direction, a macroscopic polarization may arise in the material.

In order to investigate the electric field columnar alignment of the Col_h liquid crystalline phase of **4**, the samples were introduced by capillarity into a Linkam sandwich-type glass cell composed of transparent ITO electrodes separated with a gap of 5 μm. Then, texture changes as a function of temperature, in the presence of electric fields with varying frequency and voltage, were recorded by POM at the glass-ITO interface (Fig. 5e). When the LC sample was cooled from the isotropic liquid to the columnar mesophase in the absence of electric field, the expected texture developed homogeneously over the entire view, which is in agreement with the formation of columnar mesophases with different domain orientations, as observed by AFM. Then, heating back to the isotropic phase resulted in the disappearance of all textures, because of molecular deaggregation. Now, when cooling again while applying an electric field, textures only grew out of the electrode area, suggesting a unidirectional orientation of the columns, perpendicular to the substrate and parallel to the electric field (*i.e.* homeotropic alignment). Remarkably, this alignment was reproducible over many cycles and maintained even after the electric field was switched off, as long as the oriented sample was kept within the mesophase temperature range.

Further studies using second harmonic generation (SHG) confirmed a thermally stable electric-field-induced polar organization along the field direction, which grows as the material enters into the mesophase temperature range (Fig. 5f) and is maintained at room temperature for several weeks without degradation. In addition, the team used a different optical setup to measure SHG interferometry (Fig. 5g). The results indicated that the interference pattern of the material remains unaltered if the field is turned off or even reversed within the mesophase temperature range (red and black curves in Fig. 5g). In other words, the liquid crystal phase is permanently polarized and not electrically invertible (*i.e.* it cannot be switched), which is characteristic of pyroelectric materials. This unusual property, unprecedented for organic materials of this class, was attributed to the high amount of energy required to invert polarization, which demands to turn upside down each molecule in the ordered columns. The only way to invert the polarization of the material is to

heat back to the isotropic phase, and cool down again by applying an electric field in the opposite sense (blue curve in Fig. 5g). In short, this work nicely demonstrated how the axial dipole moment of a π -conjugated molecule can be transferred to a permanent macroscopic net polarization in a self-assembled material, as illustrated in Fig. 5h.

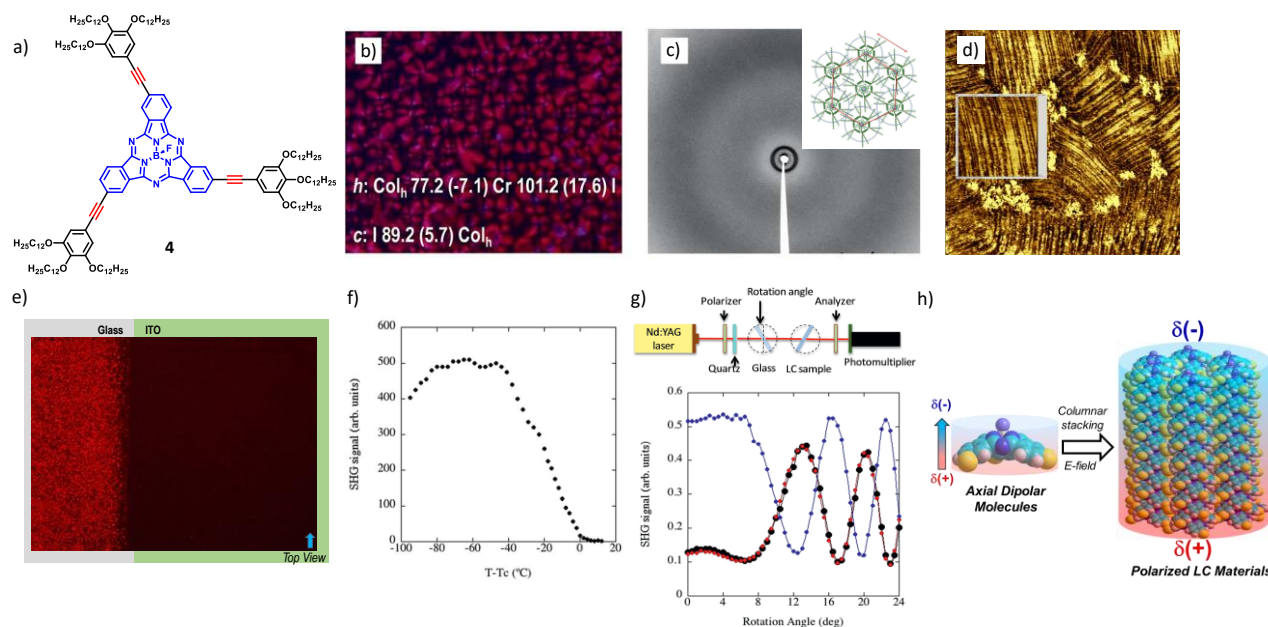


Fig. 5. (a) Molecular structure of SubPc **4**. (b) POM photograph (x50) at r.t. on cooling from the isotropic phase. Transition temperatures (°C) and enthalpy values (kJ·mol⁻¹) correspond to the second heating. (c) X-ray diffractogram at r.t. The inset shows the hexagonal columnar arrangement of the mesophase with an intercolumnar distance of about 4 nm (red arrow). (d) AFM 2D phase image of a thermally treated sample of SubPc **4** deposited onto mica. (e) POM photograph (x20, r.t.) of a 5 μm sandwich cell with ITO electrodes. An electric field was applied during the I-Col_h transition that provoked the orientation of the columns. (f) Temperature dependence of the SHG signal at an angle on incidence of 30°. (g) Scheme of the optical setup used for SHG interferometry and interference patterns at 40 °C. Blue and red points correspond to a LC sample that was polarized with (+) and (-) DC electric field, respectively, on cooling from the isotropic phase. Black points were obtained by reversing the (-) DC field without heating the sample to the isotropic phase and were found to overlap red points, meaning that the polarization of the sample was immune to the applied field. (h) Schematic representation of the axial dipole moment transfer from the π -conjugated SubPc **4** to the corresponding self-assembled π -conjugated material which displays permanent net polarization. Adapted with permission from ref. [26]. Copyright 2015 Royal Society of Chemistry.

Liquid crystalline materials with switchable polarization

Lyotropic LCs. The columnar mesophase of compound **4** does not show ferroelectric switching ability because the molecule is devoid of strong dipolar groups that can invert polarization in response to electric fields. However, the authors considered SubPc **3**, presenting three peripheral amide groups, as the next target in their studies. Since it is known that these dipolar groups can invert orientation following an applied field^[28,29], ferri- or ferroelectric materials could be obtained from their columnar LC phases. In fact, molecule **3** assembled in similar thermotropic columnar mesophases as those observed by **4**, but the transition to the isotropic liquid is situated at much higher temperatures (*i.e.* around 250 °C), as expected in view of the extra stabilization of the columns by hydrogen-bonding, which strongly hampered the obtention of reliable measurements due to partial degradation after several temperature cycles. However, the authors discovered that, upon mixing with dodecane (10 wt% / $3.4 \cdot 10^{-2}$ M solutions), the compound forms nematic columnar (N_{Col}) mesophases. Intuitively, the dodecane solvent is introduced between columns and mixed with the SubPc peripheral dodecyl tails, granting higher fluidity to the non-centrosymmetric columnar structures of **3** (see Fig. 3)^[23] and converting them into “supramolecular” nematic mesogens, in which the coexistence of π -stacking, threefold

H-bonding and dipole-dipole interactions provided the necessary stability to maintain columnar association in solution^[27].

Texture observation of the lyotropic mesophase of **3** in dodecane within glass cells with transparent ITO electrodes indicated that the material shows electro-optic response (Fig. 6a). The polar switching of the nematic phase was fully characterized by SHG and SHG interferometry. When the sample was subjected to an electric field, very strong SHG signals were observed, which saturate for fields in the range of $10 \text{ V}\mu\text{m}^{-1}$. The calculated remnant polarization (P_r) of *ca.* $0.13 \text{ }\mu\text{C}/\text{cm}^2$ is lower than the value obtained for the fan-shaped molecular system described by Takezoe and Aida^[30] and an order of magnitude less than that observed for benzene-1,3,5-tricarboxamide materials^[28,29,31]. The experimental results imply the formation of a polar structure with a degree of order that is complete for relatively modest fields (Fig. 6b), which was ascribed to the orientation of the non-centrosymmetric SubPc columns parallel to the electric field. As a matter of fact, the polarization characteristics of the SHG light indicated that the material has a macroscopic polar axis along the field direction. When the electric field was turned off, the black (homeotropically aligned) texture was retained for a few minutes and then developed into a new texture that was different from the original one (Fig. 6a; center), supposedly originated from the reorganization of the columns to cancel the net polarization. In addition, the SHG interferograms (Fig. 6c) obtained inverting the electric field demonstrated unambiguously that, in this case, positive and negative fields induced opposite polarities in the sample, indicating that the material presents polar switching, which could be partially retained when the electric field was turned off (Fig. 6c). Therefore, this material could be considered as the first nematic columnar ferroelectric phase.

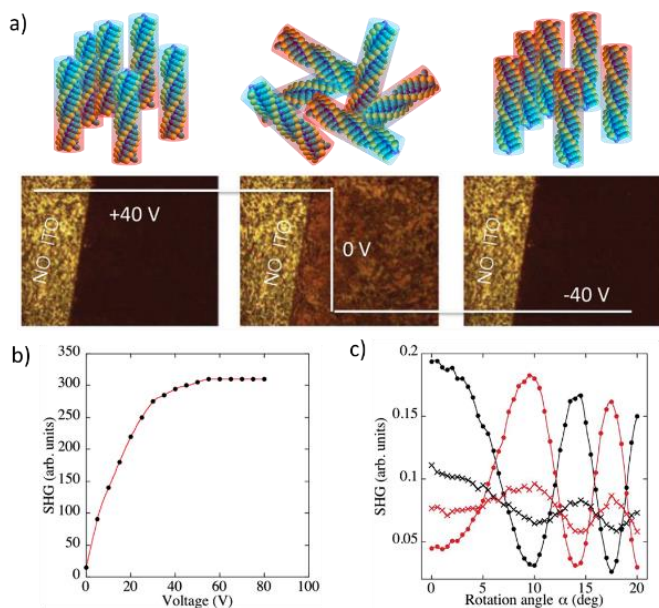


Fig. 6. (a) Schematic representation of the polar switching and textures observed by POM for the lyotropic NCol mesophase of SubPc **3** in dodecane (10 wt%) under a low-frequency (0.1 Hz) square-wave field: left, +40 V; center, transient texture observed during voltage inversion; right, -40 V. Sample thickness, 5 μm . (b) Voltage dependence of the SHG signal at an angle of incidence of 30° . (c) SHG interferograms obtained for positive (black dots) and negative (red dots) field applications ($10 \text{ V}\mu\text{m}^{-1}$), and without electric field after the pretreatment with positive and negative fields (black and red crosses). Adapted with permission from ref. [27]. Copyright 2015 Wiley-VCH Verlag GmbH & Co. KGaA.

Thermotropic LCs. As we commented before, the alignment and polarization changes of thermotropic LCs of amide-substituted SubPc **3** could not be easily studied by optical techniques like POM or SHG because of the high temperatures required to reach the isotropic liquid phase and thus achieve optimal homeotropic alignment. However, this problem could be circumvented by applying an external field of $\sim 30 \text{ V}/\mu\text{m}$ at $130\text{--}140^\circ\text{C}$ for about 20 min, which

allowed to obtain a high degree of homeotropic alignment, as demonstrated by the appearance of a black texture (Fig. 7a). This is a nice demonstration of the extra value of organic materials for device fabrication, which can be produced after a simple combination of solution processing and field annealing. Using this alignment procedure, Kemerink *et al.* developed an unprecedented and promising system able to modulate material conductivity using the large electric fields associated with ferroelectric polarization^[32].

SubPc **3** is endowed with a semiconducting π -conjugated core surrounded by dipolar amide side groups that are responsible for the formation of a hydrogen-bonded network along the columns and that can reorient in response to applied electric fields, potentially changing the net polarization of the whole column. Through this design, the authors described the first organic material in which charge transport is coupled to ferroelectric polarization. So, the authors described that the supramolecular organization of the SubPc **3** (Fig. 3a) provides long-range polar order that supports collective ferroelectric behavior of the side groups, as well as charge transport through the stacked semiconducting cores. Simultaneous switching of polarization and conductivity measurements of organic ferroelectric semiconductor (oFESC, Fig. 7b-c) devices, based on LCs of SubPc **3** sandwiched between gold electrodes, indicated a polarization reversal when the externally applied electric field passes the coercive field, as well as a strong rectifying behavior at low voltages. These experiments displayed a remarkable and unprecedented hysteresis behavior in the current-voltage (j V) loop which is attributed to a bulk conductivity modulation. In other words, the material switches from a high conductivity state, when polarization and conductivity are parallel, to a low conductivity state, when they are antiparallel (Fig. 7d).

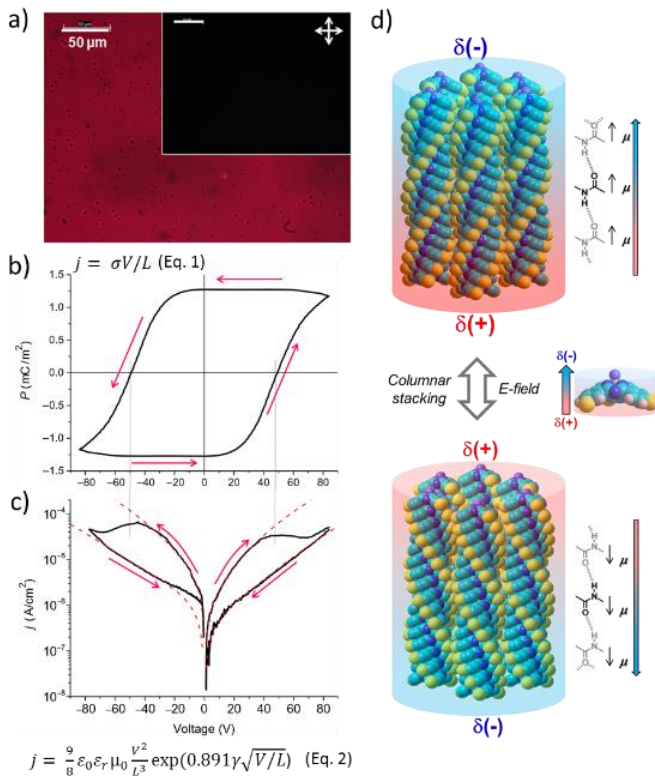


Fig. 7. (a) oFESC device. The inset shows the device after the electric-field alignment procedure at 135-140 °C and cooling down. The complete darkness indicates a stable homeotropic out-of-plane orientation. (b) Ferroelectric polarization and (c) current versus applied voltage for a Au/SubPc-amide/Au diode. Polarization and current are separate measurements on the same device. Thin dotted lines indicate the coercive voltage; red dashed lines are fits to a sum of ohmic and SCLC contributions, showing that conductivity is bulk-limited. Arrows indicate loop sense. Device film thickness $L = 1$ mm, $T = 130^\circ$ to 135° °C. (d) Schematic representation of the self-assembled liquid crystalline ferroelectric material in which the polarization, which can be switched as a function of the direction

of the array of hydrogen-bonded amide groups, is coupled to electron transport, and leads to a bulk switchable and rectifying conductivity. Adapted with permission from ref. [32]. Copyright 2017 American Association for the Advancement of Science.

To monitor and verify the correlation between polarization reversal and the change in conductivity, the retention of the polarization and conductivity states were investigated. The corresponding decay curves at the same rate allowed to conclude that ferroelectric polarization in the supramolecular polymers is strongly coupled to charge transport, leading to a bulk conductivity that, as the authors also experimentally demonstrated, is both switchable and rectifying. Although this was known for inorganic materials^[33], the mechanism and principles are totally different in the present system. The same study was also performed with other organic semiconductors, like phthalocyanines or perylene diimides with totally different peripheral oligo(vinylidene-difluoride) dipolar groups. Very similar results were obtained, which can be explained quantitatively by a simple two-site model for hopping charge carriers.

CONCLUSIONS

In this small review that mainly summarizes the content of four research articles we have demonstrated the potential of non-planar non-racemizable molecules with strong axial dipoles, of which SubPcs represents the only case described so far to our knowledge, to generate polarly ordered systems and materials. When piled up in non-centrosymmetric columnar nanostructures, the axial dipole moments sum up to generate systems and materials with a net polarization. Electric-field induced orientation of these self-assembled columns has been demonstrated in solution (*i.e.* lyotropic mesophases) and in the condensed stated (*i.e.* thermotropic mesophases). Furthermore, depending on the presence or absence of other axially dipolar moieties that can rearrange in response to the direction of the electric field, like hydrogen-bonded amide groups, unprecedented switchable or permanently polarized materials, respectively, can be generated. It was also demonstrated that in such materials charge conductivity can be coupled to ferroelectric polarization, increasing or decreasing depending on their parallel or antiparallel relative arrangements.

Acknowledgements

We would like to thank all collaborators who enthusiastically contributed to the development of the science presented in this review. Funding from MINECO CTQ2017-84727-P (DGR) and CTQ2017-85393-P (TT) is gratefully acknowledged.

REFERENCES

1. Wang L, Huang D, Lam L, Cheng Z. *Liquid Crystals Today*, 2017; **26**: 85–111.
2. For excellent reviews on columnar liquid crystals see: (a) Sergeyev S, Pisula W, Geerts YH. *Chem. Soc. Rev.* 2007; **36**: 1902–1929. (b) Laschat S, Baro A, Steinke N, Giesselmann F, Hägele C, Scalia G, Judele R, Kapatsina E, Sauer S, Schreivogel A, Tosoni M. *Angew. Chem. Int. Ed.* 2007; **46**: 4832–4887. (c) Kaafarani BR. *Chem. Mater.* 2011; **23**: 378–396. (d) Wöhrle T, Wurzbach I, Kirres J, Kostidou A, Kapernaum N, Litterscheidt J, Haenle JC, Staffeld P, Baro A, Giesselmann F, Laschat S. *Chem. Rev.* 2016; **116**: 1139–1241.
3. Shoyama K, Schmidt D, Mahl M, Würthner F. *Org. Lett.* 2017; **19**: 5328–5331.
4. (a) Pisula W, Feng X, Müllen K. *Adv. Mater.* 2010; **22**: 3634–3649. (b) Kumar S. *Chemistry of Discotic Liquid Crystals. From Monomers to Polymers*. CRC Press. Taylor & Francis Group.: New York, 2011.

5. (a) Hoebein FJM, Jonkheijm P, Meijer EW, Schenning APHJ. *Chem. Rev.* 2005; **105**: 1491–1546. (b) González-Rodríguez D, Schenning APHJ. *Chem. Mater.* 2011; **23**: 310–325. (c) Aida T, Meijer EW, Stupp SI. *Science* 2012; **335**: 813–817.
6. The term “cone-shaped discotic”, or also “bowlic / pyramidic” was coined in 1985 by Zimmerman and Collet. See: (a) Zimmermann H, Poupko R, Luz Z, Billard JZ. *Naturforsch.* 1985; **40a**: 149–160. (b) Malthete J, Collet A. *Nouv. J. Chim.* 1985; **9**: 151–153.
7. Claessens CG, González-Rodríguez D, Iglesias RS and Torres T. *C. R. Chimie.* 2006; **9**: 1094–1099.
8. (a) Shimizu S, Miura A, Khene S, Nyokong T, Kobayashi N. *J. Am. Chem. Soc.* 2011; **133**: 17322–17328. (b) Markopoulos G, Henneicke L, Shen J, Okamoto Y, Jones PG, Hopf H. *Angew. Chem. Int. Ed.* 2012; **51**: 12884–12887.
9. Sato K, Itoh Y, Aida T. *Chem. Sci.* 2014; **5**: 136–140.
10. Palmans AR, Meijer EW. *Angew. Chem. Int. Ed.* 2007; **46**: 8948–8969.
11. (a) Takezoe H, Kishikawa K, Gorecka E. *J. Mater. Chem.* 2006; **16**: 2412–2416. (b) Horiuchi S, Tokura Y. *Nat. Mater.* 2008; **7**: 357–361. (c) Takezoe H, Araoka F. *Liq. Cryst.* 2013; **41**: 393–401. (d) Tayi AS, Kaeser A, Matsumoto M, Aida T, Stupp SI. *Nat. Chem.* 2015; **7**: 281–294.
12. (a) Claessens CG, González-Rodríguez D, Torres T. *Chem. Rev.* 2002; **102**: 835–853. (b) Claessens CG, Gonzalez-Rodríguez D, Rodríguez-Morgade MS, Medina A, Torres T. *Chem. Rev.* 2014; **114**: 2192–2277. (c) Shimizu S, Kobayashi N. *Chem. Commun.* 2014; **50**: 6949–6966. (d) Claessens CG, Torres T. *Angew. Chem. Int. Ed.* 2002; **41**: 2561–2565.
13. Samdal S, Volden HV, Ferro VR, García de la Vega JM, González-Rodríguez D, Torres T. *J. Phys. Chem. A* 2007; **111**: 4542–4550.
14. (a) Malthete J, Collet A. *J. Am. Chem. Soc.* 1987; **109**: 7544–7545. (b) Zimmermann H, Tolstoy P, Limbach HH, Poupko R, Luz Z. *J. Phys. Chem. B* 2004; **108**: 18772–18778. (c) Lovas FJ, McMahon RJ, Grabow JU, Schnell M, Mack J, Scott LT, Kuczkowski RL. *J. Am. Chem. Soc.* 2005; **127**: 4345–4349.
15. (a) Guilleme J, González-Rodríguez D, Torres T. *Angew. Chem. Int. Ed.* 2011; **50**: 3506–3509. (b) Guilleme J, Martínez-Fernandez L, González-Rodríguez D, Corral I, Yañez M, Torres T. *J. Am. Chem. Soc.* 2014; **136**: 14289–14298. (c) Guilleme J, Martínez-Fernandez L, Corral I, Yañez M, González-Rodríguez D, Torres T. *Org. Lett.* 2015; **17**: 4722–4725. (d) González-Rodríguez D, Claessens CG, Torres T. *J. Porphyr. Phthalocyanines* 2009; **13**: 203–214.
16. Claessens CG, González-Rodríguez D, Torres T, Martín G, Agulló-López F, Ledoux I, Zyss J, Ferro VR, García de la Vega JM. *J. Phys. Chem.* 2005 ; **109**: 3800–3806.
17. (a) Spesia MB, Durantini EN. *Dyes Pigm.* 2008; **77**: 229–237. (b) Xu H, Jiang XJ, Chan, EYM, Fong WP, Ng DKP. *Org. Biomol. Chem.* 2007; **5**: 3987–3992. (c) Van de Winckel E, de la Escosura A, Torres T. *Org. Chem. Res.* 2017; **3**, 1–7. (d) Van de Winckel E, Mascaraque M, Zamarrón A, Juarranz de la Fuente A, Torres T, de la Escosura A. *Adv. Funct. Mater.* 2018; **28**: 1705938. (e) Almeida-Marrero V, van de Winckel E, Anaya-Plaza E, Torres T, de la Escosura A, *Chem. Soc. Rev.* 2018; **47**: 7369–7400.
18. (a) González-Rodríguez D, Torres T, Guldi DM, Rivera J, Echegoyen L. *Org. Lett.* 2002; **4**: 335–338. (b) González-Rodríguez D, Torres T, Olmstead MM, Rivera J, Herranz MA, Echegoyen L, Atienza-Castellanos C, Guldi DM. *J. Am. Chem. Soc.* 2006; **128**: 10680–10681. (c) González-Rodríguez D, Carbonell E, Guldi DM, Torres T. *Angew. Chem. Int. Ed.* 2009; **48**: 8032–8036. (d) González-Rodríguez D, Carbonell E, Rojas GdM, Castellanos CA, Guldi DM, Torres T. *J. Am. Chem. Soc.* 2010; **132**: 16488–16500. (e) Romero-Nieto C,

- Guilleme J, Fernández-Ariza J, Rodríguez-Morgade M S, González-Rodríguez D, Torres T, Guldi DM. *Org. Lett.* 2012; **14**: 5656–5659. (f) Romero-Nieto C, Guilleme J, Villegas C, Delgado JL, González-Rodríguez D, Martín M, Torres T, Guldi DM. *J. Mater. Chem.* 2011; **21**: 15914–15918.
19. (a) Morse G.E, Bender TP. *ACS Appl. Mater. Interfaces* 2012; **4**: 5055–5068. (b) Menke SM, Luhman WA, Holmes R J. *Nature Mater.* 2012; **12**: 152–157. (c) Cnops K, Rand BP, Cheyins D, Verreet B, Empl MA, Heremans P. *Nature Commun.* 2014; **5**: 3406. (d) Cnops K, Zango G, Genoe J, Heremans P, Martinez-Diaz MV, Torres T, Cheyins D. *J. Am. Chem. Soc.* 2015; **137**: 8991–8997. (e) Urbani M, Aslihan Sari F, Grätzel M, Nazeeruddin MK, Torres T, Ince M. *Chem. Asian J.* 2016; **11**: 1223–1231. (f) Josey DS, Nyikos SR, Garner RK, Dovijarski A, Castrucci JS, Wang JM, Evans GJ, Bender TP. *ACS Energy Lett.* 2017; **2**: 726–732. (g) De la Torre G, Bottari G, Torres T. *Adv. Energy Mater.* 2017; **7**: 1601700. (h) Duan D, Zango G, García-Iglesias M, Colberts FJM, Wienk MM, Martínez-Díaz MV, Janssen RAJ, Torres T. *Angew. Chem. Int. Ed.* 2017; **56**: 148 –152. (i) de la Torre G, Bottari G, Hahn U, Torres T. *Structure and Bonding*, 2010; **135**: 1-44. (j) Verreet B, Rand BP, Cheyins D, Hadipour A, Aernouts T, Heremans P, Medina, A, Claessens CG, Torres T. *Adv. Ener. Mat.* 2011; **1**: 565–568. (k) Diaz-Diaz D, Bolink HJ, Cappelli L, Claessens CG, Coronado E, Torres T. *Tetrahedron Lett.* 2007; **48**: 4657–4660. (l) González-Rodríguez D, Carbonell E, de Miguel Rojas G, Atienza Castellanos C, Guldi DM, Torres, T. *J. Am. Chem. Soc.* 2010; **132**: 16488–16500.
 20. Rodríguez-Morgade MS, Claessens CG, Medina A, González-Rodríguez D, Gutiérrez-Puebla E, Monge A, Alkorta I, Elguero J, Torres T. *Chem. Eur. J.* 2008; **14**: 1342–1350.
 21. Shimizu S, Nakano S, Kojima A, Kobayashi N. *Angew. Chem. Int. Ed.* 2014; **53**: 2408 –2412.
 22. Shimizu S, Kobayashi N. *Chem. Commun.* 2014; **50**: 6949–6966.
 23. Guilleme J, Mayoral MJ, Calbo J, Aragón J, Viruela PM, Ortí E, Torres T, González-Rodríguez D. *Angew. Chem. Int. Ed.* 2015; **54**: 2543–2547.
 24. Shimizu S, Miura A, Khene S, Nyokong T, Kobayashi N. *J. Am. Chem. Soc.* 2011; **133**: 17322–17328.
 25. Calvo J. *Supramol. Chem.* 2018; **30**: 876–890.
 26. Guilleme J, Aragón J, Ortí E, Caverio E, Sierra T, Ortega J, Folcia CL, Etxebarria J, González-Rodríguez D, Torres T. *J. Mater. Chem. C*, 2015; **3**: 985–989.
 27. Guilleme J, Caverio E, Sierra T, Ortega J, Folcia CL, Etxebarria J, Torres T, González-Rodríguez D. *Adv. Mater.* 2015; **27**: 4280–4284.
 28. Fitié CFC, Roelofs WSC, Kemerink M, Sijbesma RP. *J. Am. Chem. Soc.* 2010; **132**: 6892–6893.
 29. Fitié CFC, Roelofs WSC, Magusin PCMM, Wübberhorst M, Kemerink M, Sijbesma RP. *J. Phys. Chem. B* 2012; **116**: 3928–3937.
 30. (a) Miyajima D, Araoka F, Takezoe H, Kim J, Kato K, Takata M, Aida T. *Science* 2012; **336**: 209–213. (b) Araoka F, Takezoe H. *Jpn. J. Appl. Phys.* 2014; **53**: 01AA01.
 31. Gorbunov AV, Putzeys T, Urbanavičiūtė I, Janssen RAJ, Wübberhorst M, Sijbesma RP, Kemerink M. *Phys. Chem. Chem. Phys.* 2016; **18**: 23663–23672.
 32. Gorbunov AV, García Iglesias M, Guilleme J, Cornelissen TD, Roelofs WSC, Torres T, González-Rodríguez D, Meijer EW, Kemerink M. *Sci. Adv.* 2017; **3**: e1701017.
 33. Choi T, Lee S, Choi YJ, Kiryukhin V, Cheong SW. *Science* 2009; **324**: 63–66.